

Hot-cold plasma transition region: collisionless case

M. Karlický¹ and F. Karlický²

¹ Astronomical Institute of the Czech Academy of Sciences, Fričova 298, CZ – 251 65 Ondřejov, Czech Republic

² Department of Physics, Faculty of Science, University of Ostrava, 30 dubna 22, 701 03 Ostrava, Czech Republic

Received ; accepted

ABSTRACT

Aims. We study processes at the transition region between hot (rare) and cold (dense) plasma in the collisionless regime.

Methods. We use a 3-dimensional electromagnetic particle-in-cell (3-D PIC) relativistic code.

Results. We initiate a transition region between the hot (rare) and cold (dense) plasma. Motivated by the transition region in the solar atmosphere the temperature and density ratio of the plasmas is chosen as 100 and 0.01, respectively. For better understanding of studied processes we make two types of computations: a) without any interactions among plasma particles (free expansion) and b) with the full electromagnetic interactions (but no particle-particle collisions). In both the cases we found that the flux of cold plasma electrons and protons from colder plasma to hotter one dominates over the flux of hot plasma electrons and protons in the opposite direction. Thus, the plasma in the hotter part of the system becomes colder and denser during time evolution. In the case without any interactions among particles the cold plasma electrons and protons freely penetrate into the hot plasma. But, the cold plasma electrons are faster than cold plasma protons and therefore they penetrate deeper into the hotter part of the system than the protons. Thus, the cooling of the electron and proton components of the plasma in the hotter part of the system is different. On the other hand, in the case with the electromagnetic interactions, owing to the plasma property, which tries to keep the total electric current constant everywhere (close to zero in our case), the cold plasma electrons penetrate into the hotter part of the system together with the cold plasma protons. Thus, the cooling of the hotter plasma is much slower and it is the same for electrons and protons. Moreover, the plasma waves generated at the transition region during these processes reduce the number of electrons escaping from the hot plasma into the colder one and scatter the cold plasma particles penetrating to the hot plasma. Therefore these waves support a temperature jump between hot and cold plasma. Nevertheless, for stabilizing of this temperature jump as in the real solar transition region, we propose that the gravity force and more or less permanent heating source in the corona (nanoflares?) together with the appropriate radiative losses at both sides of the transition region need to be included. In our case it is interesting that just in front of the expanding cold plasma to hotter one the formed electric field is opposite to that found in the case of the plasma expansion into vacuum or in the case of the plasma expansion to plasma with lower density, but having the same temperature. We propose that it is caused by a high temperature difference between hot and cold plasmas at the transition region.

Key words. Plasmas — Sun: transition region

1. INTRODUCTION

In the solar atmosphere there is a layer between the relatively cool chromosphere (≈ 10000 K) and hot corona (≥ 1 MK) which is called the transition region. Although in models of the solar atmosphere the transition region is described as the smooth interface between the chromosphere and corona, in reality it is a highly dynamic place, where a cool chromospheric material protrudes (such as prominences) or shoots out into the corona (as observed in spicules and surges) (Mariska 1992; Peter 2002a,b; Judge 2008; Zacharias et al. 2009).

The problem of the solar transition region is closely connected with the problem of the coronal heating. Many models explaining the coronal heating were proposed: a) stressing and reconnection models (e.g. Parker 1988; Heyvaerts & Priest 1992; Sturrock 1999; Gudiksen & Nordlund 2002), wave models (e.g. Kuperus et al. 1981; Hollweg & Johnson 1988;

Goossens et al. 1995; Dmitruk et al. 2002), and velocity filtration models (e.g. Scudder 1994). Moreover, Singh (2015) presented the model, where the electron accelerated in the chromospheric magnetic reconnection are further accelerated in double layers (formed in an expanding plasma) and thus heat the corona.

There are also many magnetohydrodynamic models of the transition region: static, steady flow or dynamic models, for their review, see the book of Mariska (1992). Such types of models were further evolved. For example, Zacharias et al. (2011) compared model velocities with the observed Doppler shifts of the transition emission lines. Furthermore, Ptitsyna & Somov (2012) tried to explain the observed extreme ultraviolet radiation from the transition region, and Bessalov & Savina (2015a,b) studied effects of the anomalous thermal conductivity and collective plasma processes on the structure of the transition region.

However, the transition region is very narrow. Its thickness is estimated as a few hundred kilometers, which is comparable to Coulomb mean free path for electrons and

Send offprint requests to: , e-mail: karlicky@asu.cas.cz

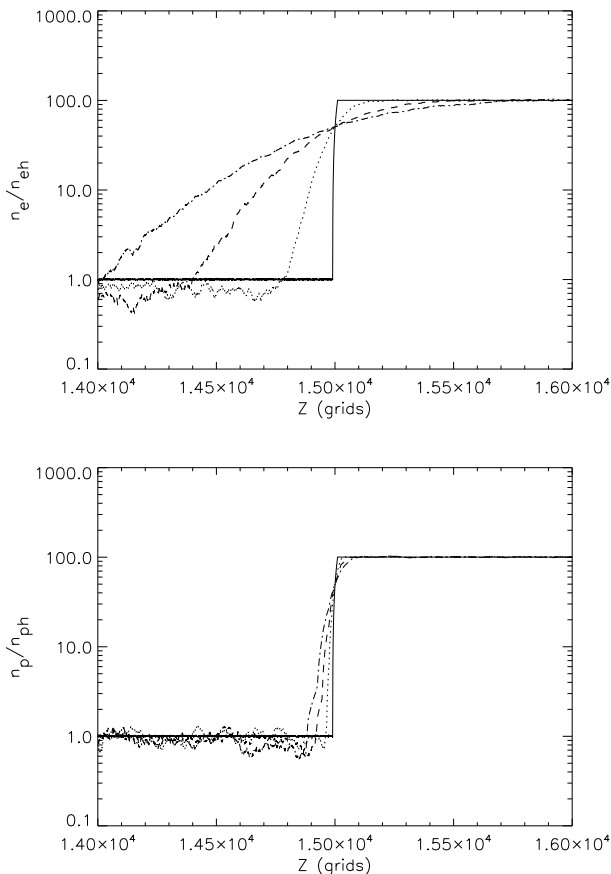


Fig. 1. Upper part: Ratio of the electron density n_e to that of the hot plasma n_{eh} along the z -coordinate at the initial state (solid line), at $\omega_{pe}t = 500$ (dotted line), at $\omega_{pe}t = 1500$ (dashed line), and at $\omega_{pe}t = 2500$ (dash-dot line). Bottom part: The same for protons. (Run with the free expansion of particles.)

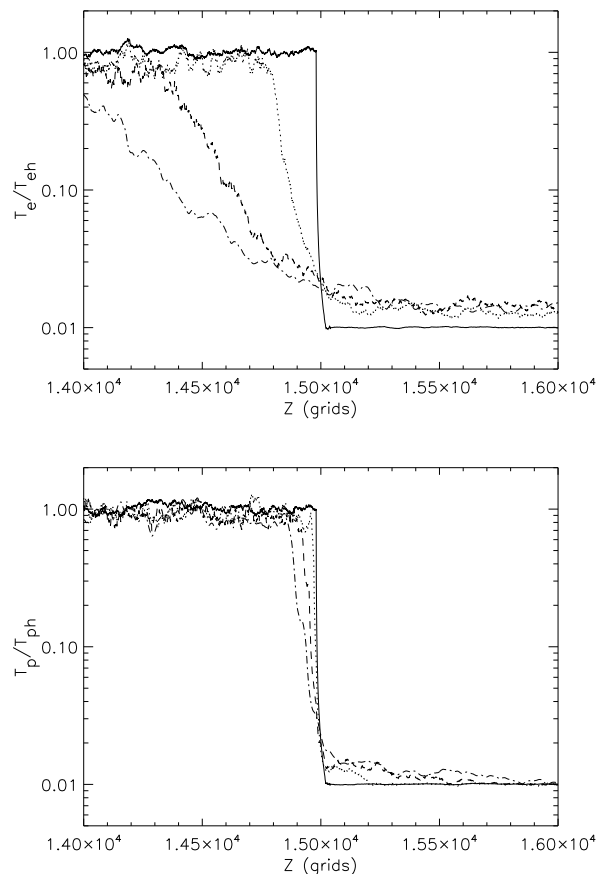


Fig. 2. Upper part: Ratio of the electron kinetic energy T (pseudo-temperature) to that of the hot plasma T_h along the z -coordinate at the initial state (solid line), at $\omega_{pe}t = 500$ (dotted line), at $\omega_{pe}t = 1500$ (dashed line), and at $\omega_{pe}t = 2500$ (dash-dot line). Bottom part: The same for protons. (Run with the free expansion of particles.)

protons (Benz 1993). Therefore, collisionless effects can be expected.

Due to the narrowness and highly dynamic state of the transition region the processes forming the transition region are not still well understood (Golub & Pasachoff 2014). Moreover, considering the problem of thermal fronts in astrophysical plasmas (Karlický 2015), there appears a question if the solar transition region is not some kind of the thermal front or cascade of thermal fronts.

For these reasons, in the present paper we study processes in the hot-cold transition region using the 3-dimensional electromagnetic particle-in-cell (PIC) relativistic model, where only collisionless processes are included. We hope that such a study helps to understand processes in the transition region.

The paper is structured as follows: In Section 2 the numerical model is described. The results are presented in section 3, Finally, discussion and conclusions are in Section 4.

2. NUMERICAL MODEL

In the model we study an interaction between the hot (rare) and cold (dense) plasma. We consider the collisionless case, i.e., the case with the particle-wave interactions only.

We use a three-dimensional (3-D) electromagnetic relativistic particle-in-cell (PIC) model (Karlický 2009) in order to include the both electrostatic and electromagnetic effects. Namely, in our study of the similar problem (problem of the thermal conduction front) we recognized an importance of the electromagnetic processes (Karlický 2015).

The system size is $L_x = 8\Delta$, $L_y = 8\Delta$ and $L_z = 30000\Delta$ (where Δ is the grid size). Thus, the system is effectively one-dimensional along the assumed magnetic field. In the model we initiate the electron-proton plasma with the proton-electron mass ratio $m_p/m_e=100$. This value is chosen to accelerate processes connected with protons. Nevertheless the ratio is still sufficient to clearly separate the dynamics of electrons and protons.

The numerical system is divided into two parts with the hot (rare) plasma (located at $z = 0 - 15000\Delta$) and cold (dense) plasma ($z = 15000 - 30000\Delta$). In the initial state the velocities of particles in the both parts of the system are described by the Maxwellian distribution functions. In the colder plasma the electron thermal velocity is chosen as $v_{T_{ec}} = 0.025 c$, where c is the speed of light. The corresponding temperature is $T_c = v_{T_{ec}}^2 m_e / (2k_B) = 1.85$ MK, where k_B is Boltzmann constant. On the other hand, the the electron thermal velocity in the hot plasma is 10 times greater (the

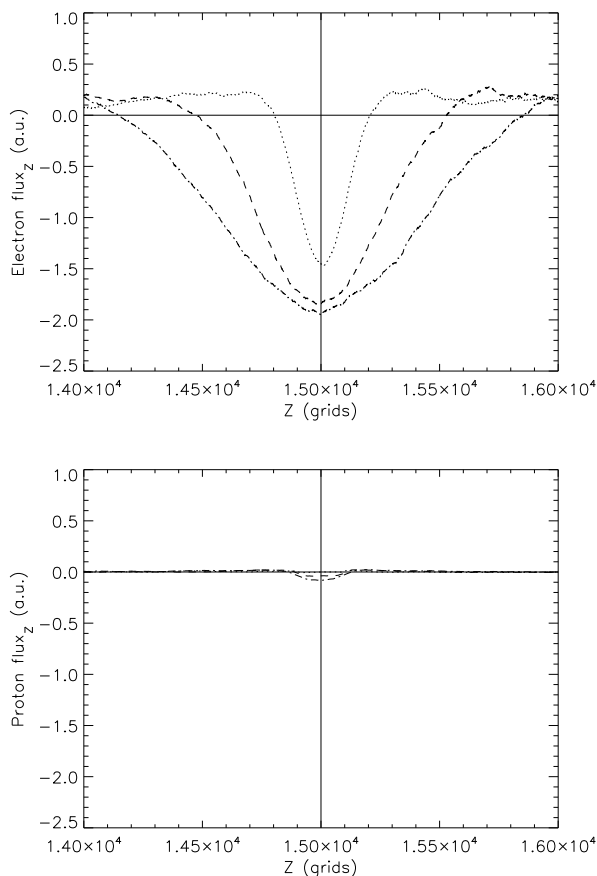


Fig. 3. Upper part: Electron flux along the z -coordinate at $\omega_{pe}t = 500$ (dotted line), at $\omega_{pe}t = 1500$ (dashed line), and at $\omega_{pe}t = 2500$ (dash-dot line). Bottom part: The same for proton flux. (Run with the free expansion of particles.)

temperature is 100 times greater = $T_h = 185$ MK) than that in the cold plasma. Thus, the ratio of temperatures in the hot and cold plasmas agrees to that in the solar transition region, but the temperatures are much higher than in the corona and chromosphere. Such a selection of temperatures is given by requirements of the PIC modelling, namely the electrostatic and electromagnetic waves in the system need to be correctly described. The initial temperatures of protons in the both parts of the system are the same as for electrons.

To simulate conditions as in the solar transition region with the pressure equilibrium we take 30 electrons and 30 protons per cube grid in the hot plasma part and 3000 electrons and 3000 protons per cube grid in the cold plasma part of the system. Note that this difference in particle densities and extension of the system for sufficient distances for particle propagations require very powerful computer.

The plasma frequency in the cold and dense plasma is $\omega_{pe} = 2\pi/t_p = 0.05$, where t_p is the plasma period. The magnetic field is oriented in z -direction and its value corresponds to the electron gyro-frequency $\omega_{ce} = 0.1 \omega_{pe}$. In the hot (rare) plasma the plasma frequency is ten times lower than that in the cold (dense) plasma. The time step is $\Delta t = 1$. The electron Debye length in the hot plasma part is $\lambda_D = 2.5 \Delta$ and in the cold plasma part $\lambda_D = 0.25 \Delta$, respectively. In the x - and y -directions the periodic boundary

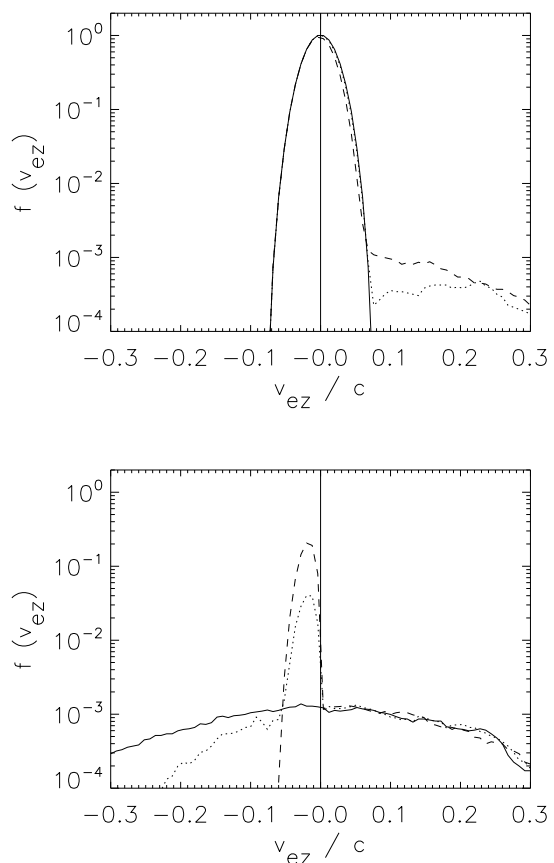


Fig. 4. Upper part: Electron distribution in the v_{ez} velocity (normalized to the distribution maximum) in the z -direction (c means the speed of light) in the space interval 15000 - 16000 grids at the initial state (solid line), at $\omega_{pe}t = 500$ (dotted line), and at $\omega_{pe}t = 2500$ (dashed line). Bottom part: Electron distribution in the v_{ez} velocity (normalized to the distribution maximum from the upper part) in the z -direction (c means the speed of light) in the space interval 14000 - 15000 grids at the initial state (solid line), at $\omega_{pe}t = 500$ (dotted line), and at $\omega_{pe}t = 2500$ (dashed line). (Run with the free expansion of particles.)

conditions are used. In the z -direction we used free boundary conditions.

Computations were performed at the IT4Innovations National Supercomputing Center, Ostrava, Czech Republic.

3. Results

To understand processes in the transition region between hot and cold plasma we made two types of computations: a) without any interactions (free expansion of particles) and b) with the electrostatic and electromagnetic (particle-wave) interactions.

Results of the computation with the free expansion of particles are presented in Figures 1 - 4. Figure 1 shows a time evolution of the electron density, normalized to the initial density in the hot plasma, along the z -coordinate in the region close to the temperature (density) jump, at times $\omega_{pe}t = 500$, $\omega_{pe}t = 1500$, and $\omega_{pe}t = 2500$, where ω_{pe} here and in the following means the plasma frequency in the

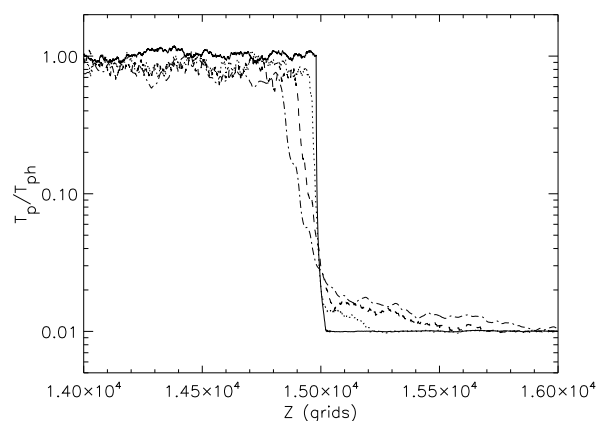
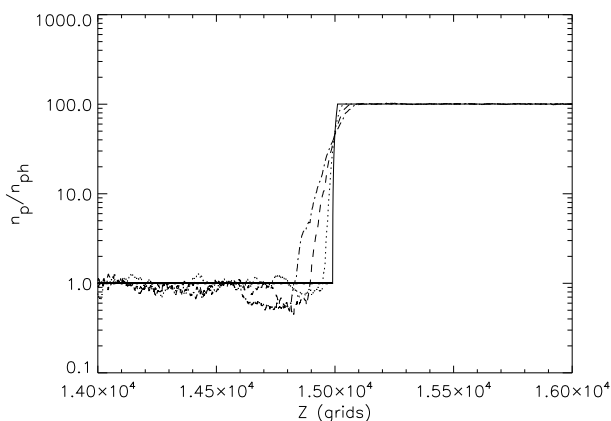
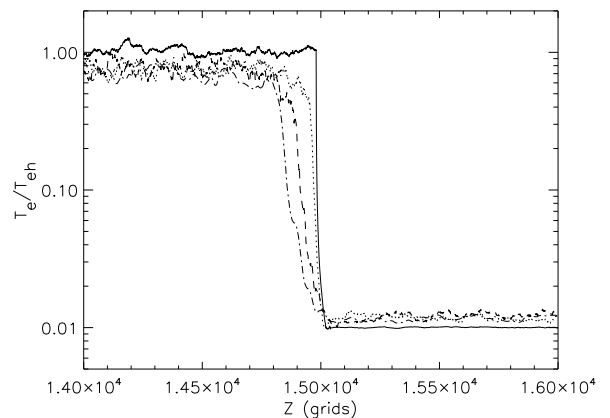
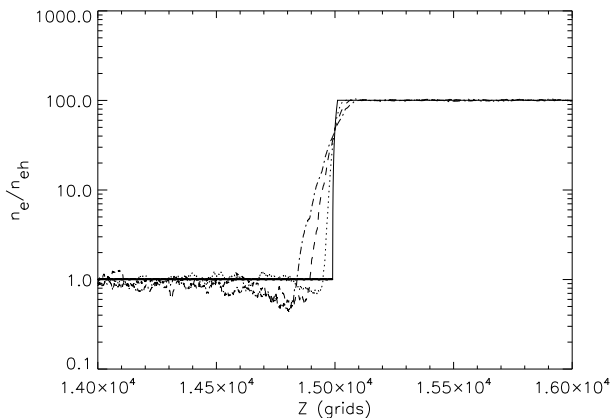


Fig. 5. Upper part: Ratio of the electron density n_e to that of the hot plasma n_{eh} along the z -coordinate at the initial state (solid line), at $\omega_{pe}t = 500$ (dotted line), at $\omega_{pe}t = 1500$ (dashed line), and at $\omega_{pe}t = 2500$ (dash-dot line). Bottom part: The same for protons. (Run with electromagnetic interactions.)

Fig. 6. Upper part: Ratio of the electron kinetic energy T (pseudo-temperature) to that of the hot plasma T_h along the z -coordinate at the initial state (solid line), at $\omega_{pe}t = 500$ (dotted line), at $\omega_{pe}t = 1500$ (dashed line), and at $\omega_{pe}t = 2500$ (dash-dot line). Bottom part: The same for protons. (Run with electromagnetic interactions.)

cold (dense) plasma. The upper and bottom parts of the figure show the evolution of the electron and proton densities. The corresponding evolution of the electron energies (pseudo-temperatures because particle distributions near the transition region deviate from the Maxwellian ones) is shown in Figure 2. Although the thermal velocities of electrons and protons in the hot plasma are in the initial state 10 times greater than those in the cold plasma, electrons as well as protons mainly flow from the colder (denser) plasma to hotter (rarer) plasma. It is due to that the electrons and protons in the cold plasma are 100 times more numerous, see the negative electron and proton flux in Figure 3. Thus, the electron and proton densities at the hotter part of the system close to the transition region increase and their temperatures decrease. Because the velocities of the cold plasma electrons are greater than those of the cold plasma protons, the electron flux is greater than the proton flux (Figure 3). See also that the cold plasma electrons penetrate deeper into the hot part of the system. It is due to that in such computations there are no particle-particle and particle-wave interactions.

But, simultaneously with the above described process the fast electrons from the hot part of the system penetrate into the region with the cold plasma, see the time evolution of the tail of the distribution function of electron

velocities in the z direction in space $z = 15000 - 16000$ grids (distribution tails in the velocity interval $v_{ez}/c = 0.1 - 0.3$) (Figure 4, upper part). On the other hand, in Figure 4 (bottom part) we can see a penetration of cold plasma electrons into the hot part of the system; compare the distribution functions in the initial state and those in the following times. The decrease of the hot plasma electrons with the negative velocities ($v_{ez}/c = -0.3 - -0.1$) in the region $z = 14000 - 15000$ grids, at $\omega_{pe}t = 500$ (dotted line) and at $\omega_{pe}t = 2500$ (dashed line) (Figure 4, bottom part) is caused by an escape of the electrons with such velocities from this region to the region with more negative locations and by a shortage of the electrons with such velocities on the cold side of the transition region.

Now, let us compare these results with those computed with the electrostatic and electromagnetic interactions (Figures 5 - 8). Similarly as in the case without any interactions there is the negative electron and proton flow from the cold to hot part of the system (Figure 7). However now, contrary to the previous case, the electron and proton flux is nearly the same and corresponds roughly to the proton flux as in the case with the free expansion of particles. It is due to that the plasma tries to keep the constant electric current density (in our case the zero initial current

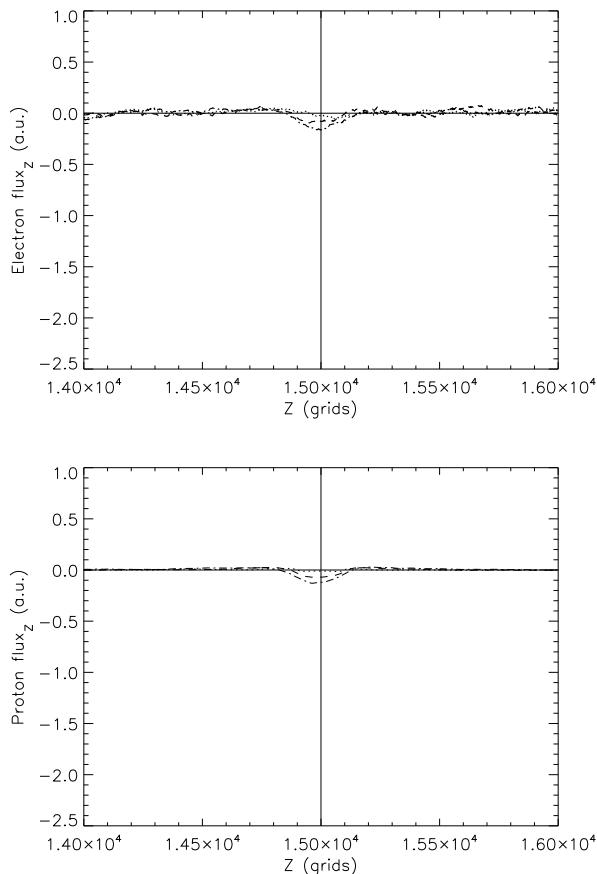


Fig. 7. Upper part: Electron flux along the z -coordinate at $\omega_{pet} = 500$ (dotted line), at $\omega_{pet} = 1500$ (dashed line), and at $\omega_{pet} = 2500$ (dash-dot line). Bottom part: The same for proton flux. (Run with electromagnetic interactions.)

density). In the initial state at the transition region the flux of the cold plasma electrons towards the hot plasma is higher than that of the proton flux. Thus, in the very short time at the head of the proton flow a region with a surplus of the negative charge (cold electrons are faster than cold protons) appears and also here the non-zero electric current is formed. Both these electrostatic and electromagnetic effects cause that the protons at this region are accelerated and electrons decelerated in the z -direction, in such a way that the both electron and proton fluxes are kept nearly the same (i.e., with zero electric current). Note that in the beam-plasma system the same process leads to a formation of the so called return-current (Karlický 2009). For details of these processes, see van den Oord (1990).

Because protons are much more heavier than electrons the expansion of the cold plasma electrons into the hot part of the system is much slower than in the case without any interactions, compare Figure 5 and Figure 1. Thus also a decrease of the electron temperature in the hot part of the system close to the transition region is slower than in the previous case, see Figure 6 and Figure 2.

Furthermore, Figure 8 shows time evolution of the electron distribution function in the v_{ez} velocities at the both sides of the hot-cold transition region. As seen here and in comparison with Figure 4, the electromagnetic processes, described above, reduce the penetration of cold plasma elec-

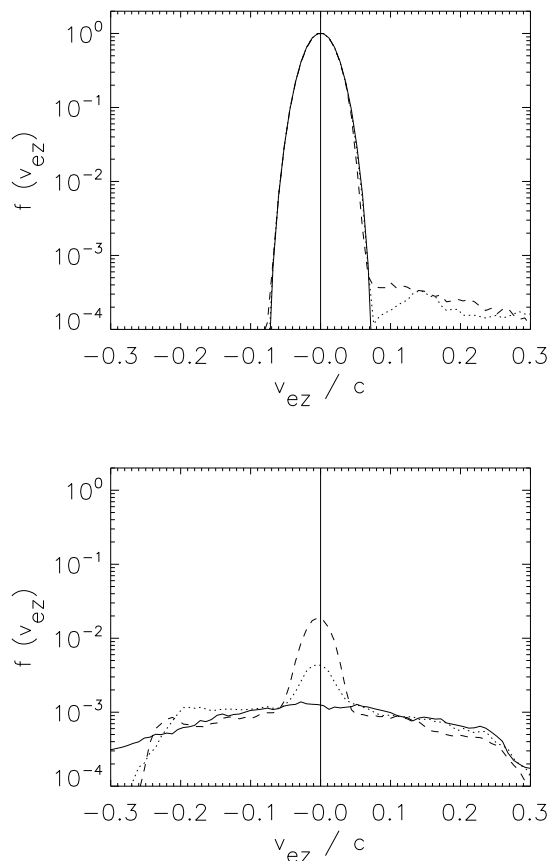


Fig. 8. Upper part: Electron distribution in the v_{ez} velocity (normalized to the distribution maximum, c means the speed of light) in the space interval 15000 - 16000 grids at the initial state (solid line), at $\omega_{pet} = 500$ (dotted line), and at $\omega_{pet} = 2500$ (dashed line). Bottom part: Electron distribution in v_{ez} velocity (normalized to the distribution maximum from the upper part) in the space interval 14000 - 15000 grids at the initial state (solid line), at $\omega_{pet} = 500$ (dotted line), and at $\omega_{pet} = 2500$ (dashed line). (Run with electromagnetic interactions.)

trons into the hot part of the system as well as the penetration of hot plasma electrons to the cold plasma region; compare Figures 8 and 4 (upper parts) in the velocity interval $v_{ez} = 0.1 - 0.3$. Even some hot plasma electrons are backscattered, see the distribution expressed by the dashed line for the velocities around $v_{ez}/c = -0.08$. This effect indicates that around the hot-cold transition region the plasma waves are generated which backscatter the hot plasma electrons. Another and even stronger effect of the backscattering of electrons can be seen by comparing of Figures 8 and 4, bottom parts. While in the case without any interactions the cold plasma electrons penetrating to the hot part of the system have only negative velocities, in the case with the electromagnetic interactions the cold plasma electrons have also positive velocities. The maximum of the distribution of these cold plasma electrons is slightly shifted to the negative velocities. This velocity shift corresponds to the velocity of the distribution maximum of the cold plasma protons flowing together with the electrons from cold plasma to hot plasma. The cold plasma protons in the hotter part of the

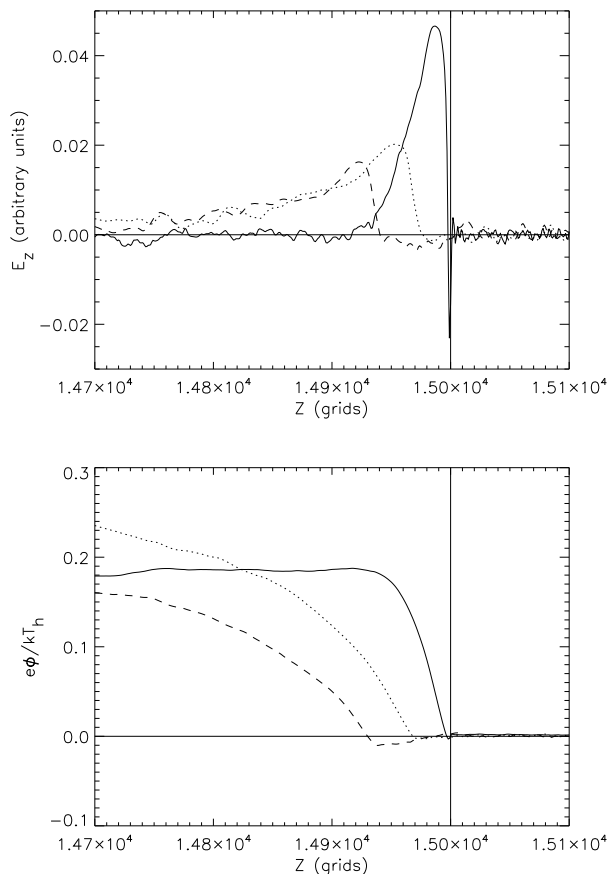


Fig. 9. Upper part: Electric field in the z -direction in the space interval 14700 - 15100 grids at $\omega_{pe}t = 25$ (solid line), at $\omega_{pe}t = 500$ (dotted line), and at $\omega_{pe}t = 1000$ (dashed line). Bottom part: Electric potential in the z -direction in the same space interval and same times. (Run with electromagnetic interactions.)

system have only negative velocities and for this short time of evolution they are only negligibly scattered.

Figure 8 (bottom part) also shows that the electron distribution in space around the hot-cold transition region is a mixture of the hot and cold plasma electrons.

We also analyzed the electric field and corresponding potential in this hot-cold plasma system. We found that except the negatively oriented electric field at the very beginning of the system evolution and in the space interval 14998-15000 grids (Figure 9, solid line in the upper part), the electric field is positively oriented and decreases in time (Figure 9, the upper part). In the bottom part of Figure 9 we present the corresponding normalized electric potential, which is about $e\phi/k_B T_h = 0.2$, where e is the electric charge, ϕ is the potential, k_B is the Boltzmann constant, and T_h is the temperature of the hot plasma.

4. Discussion and conclusions

Using the 3-D PIC model we studied processes at the transition region between hot (rare) and cold (dense) plasma. Ratios of the initial hot and cold plasma temperatures and rare and dense plasma densities were taken as 100 and 0.01, respectively, i.e., as in the case with the pressure equilibrium in the solar atmosphere. Two types of computations

were made: with and without the electromagnetic interactions.

In both the cases we found that the flow of cold plasma electrons and protons from colder plasma to hotter one is greater than that of hot plasma electrons and protons in the opposite direction. It is given by the initial conditions in the system, where the relation $n_c T_c = n_h T_h$, where n_c and n_h are the particle densities and T_c and T_h are the cold and hot plasma temperatures, is used. Note that the T_c and T_h are proportional to the square of the thermal particle velocities v_{T_c} and v_{T_h} , and the particle flux is $n_c v_{T_c}$ and $n_h v_{T_h}$, respectively.

Due to this flow the plasma in the hotter part of the system becomes colder and denser during time evolution. In the case without any interactions among particles cold plasma electrons and protons freely penetrate into the hot plasma. However, the cold plasma electrons are faster than cold plasma protons and therefore they penetrate deeper into the hotter part of the system than the protons. Therefore, the cooling of the electron and proton components of the plasma in the hotter part of the system is different. On the other hand, in the case with the electrostatic and electromagnetic interactions, owing to the plasma property which tries to keep the total electric current constant everywhere (in our system close to zero), the cold plasma electrons penetrate into the hotter part of the system together with the cold plasma protons. Thus, the cooling of the hotter plasma is much slower and it is the same for electrons and protons. Note that for the real proton-electron mass ratio (1836) the process of penetration of the cold plasma protons and electrons into the hotter part of the system will be even slower than in the present case, where we used the mass ratio equal to 100. Furthermore, the plasma waves generated during these processes reduce a number of the electrons escaping from the hot plasma into the colder one and scatter the cold plasma electrons penetrating into the hotter part of the system.

We found that except the negatively oriented electric field at the very beginning of the system evolution and in the very narrow region close to the boundary between the hot and cold plasma, the electric field is oriented in the opposite direction comparing to that of the expanding cold plasma to hotter one, and the electric field decreases in time.

Solving Vlasov equations Singh & Schunk (1982); Singh et al. (1987); Singh (2011) studied an expansion of the plasma into vacuum and expansion of the plasma into the plasma with lower density, but having the same temperature. In the both these cases the electric field was oriented in the direction of plasma expansion. It is due to that the electrons expand faster than protons. In our simulations we recognized this effect only at the very beginning of the system evolution and only in the very narrow region close to the boundary between the hot and cold plasma. But simultaneously, the another effect caused by hot plasma electrons appears. Namely, the hot electrons in the hot plasma region close to the hot-cold boundary expand to the colder plasma side and thus at this region a surplus of the positive charge appears. It produces the found electric field oriented in the opposite direction comparing to that of the expanding cold plasma to hotter one.

If we compare the processes in the present model with those in the thermal front, computed in the plasma having the constant density, (Karlický 2015), we can see that only

the process reducing a penetration of hot plasma electrons into the cold plasma (due to the plasma waves) is similar. The main difference is given by a strong jump in densities of the hot and cold plasmas and corresponding flow of the cold plasma protons (together with the cold plasma electrons) from the cold (dense) plasma to hotter (rare) one.

Now a question arises if this cold proton (cold electron) flow can be stopped by some way and thus stabilize the temperature-density structure as in the real transition region in the solar atmosphere. Analyzing this problem, we think that this flow can be stopped by the gravity force together with the generated plasma waves. Namely, the flow of the cold plasma electrons and protons in the real solar atmosphere is oriented upwards, thus the gravity force can decelerate and stopped this flow.

Furthermore, we think that the temperature jump in the transition region (between the corona and chromosphere) needs some more or less permanent source of heating in the corona (probably nanoflares). On the other hand, the flow of hot plasma electrons from the corona to the chromosphere is reduced by the plasma waves generated at the transition region, as shown in these simulations. Based on our analysis of thermal fronts (Karlický 2015) we think that the flow of hot electrons to the transition region can be even more reduced, if the strong ion-sound turbulence is present at the transition region.

Finally, we found that the electron distribution in space around the hot-cold transition region is a mixture of the hot and cold plasma electrons. This can be important in interpretations of the X-ray line spectra formed at the solar transition region (Dzifčáková et al. 2017; Dudík et al. 2017).

Acknowledgements. We acknowledge support from Grants 16-13277S and 17-16447S of the Grant Agency of the Czech Republic and institutional support from the University of Ostrava (IRP201557). This work was supported by The Ministry of Education, Youth and Sports from the Large Infrastructures for Research, Experimental Development and Innovations project „IT4Innovations National Supercomputing Center – LM2015070“.

References

- Benz, A. O., ed. 1993, *Astrophysics and Space Science Library*, Vol. 184, *Plasma astrophysics: Kinetic processes in solar and stellar coronae*, Kluwer Acad. Publishers, The Netherland, p. 285
- Bespalov, P. A. & Savina, O. N. 2015a, *Central European Astrophysical Bulletin*, 39, 43
- Bespalov, P. A. & Savina, O. N. 2015b, *Astronomy Letters*, 41, 601
- Dmitruk, P., Matthaeus, W. H., Milano, L. J., et al. 2002, *ApJ*, 575, 571
- Dudík, J., Dzifčáková, E., Meyer-Vernet, N., et al. 2017, *ArXiv e-prints* [[arXiv:1706.03396](https://arxiv.org/abs/1706.03396)]
- Dzifčáková, E., Vocks, C., & Dudík, J. 2017, *A&A*, 603, A14
- Golub, L. & Pasachoff, J. M. 2014, *Nearest Star*, Cambridge Univ. Press, Cambridge, UK
- Goossens, M., Ruderman, M. S., & Hollweg, J. V. 1995, *Sol. Phys.*, 157, 75
- Gudiksen, B. V. & Nordlund, Å. 2002, *ApJ*, 572, L113
- Heyvaerts, J. & Priest, E. R. 1992, *ApJ*, 390, 297
- Hollweg, J. V. & Johnson, W. 1988, *J. Geophys. Res.*, 93, 9547
- Judge, P. 2008, *ApJ*, 683, L87
- Karlický, M. 2009, *ApJ*, 690, 189
- Karlický, M. 2015, *ApJ*, 814, 153
- Kuperus, M., Ionson, J. A., & Spicer, D. S. 1981, *ARA&A*, 19, 7
- Mariska, J. T. 1992, *The Solar Transition Region*, Cambridge Univ. Press, Cambridge, UK
- Parker, E. N. 1988, *ApJ*, 330, 474
- Peter, H. 2002a, *Advances in Space Research*, 30, 501

- Peter, H. 2002b, in *ESA Special Publication*, Vol. 508, *From Solar Min to Max: Half a Solar Cycle with SOHO*, ed. A. Wilson, 237–244
- Ptitsyna, O. V. & Somov, B. V. 2012, *Astronomy Letters*, 38, 801
- Scudder, J. D. 1994, *ApJ*, 427, 446
- Singh, N. 2011, *Physics of Plasmas*, 18, 122105
- Singh, N. 2015, *ApJ*, 810, L1
- Singh, N. & Schunk, R. W. 1982, *J. Geophys. Res.*, 87, 9154
- Singh, N., Thiemann, H., & Schunk, R. W. 1987, *Laser and Particle Beams*, 5, 233
- Sturrock, P. A. 1999, *ApJ*, 521, 451
- van den Oord, G. H. J. 1990, *A&A*, 234, 496
- Zacharias, P., Bingert, S., & Peter, H. 2009, *Mem. Soc. Astron. Italiana*, 80, 654
- Zacharias, P., Peter, H., & Bingert, S. 2011, *A&A*, 531, A97